



Contents lists available at ScienceDirect

Transportation Research Part C

journal homepage: www.elsevier.com/locate/trc

Mixed flow of autonomous and human-driven vehicles: Analytical headway modeling and optimal lane management[☆]

Reza Mohajerpoor^{a,b}, Mohsen Ramezani^{a,*}

^a The University of Sydney, School of Civil Engineering, Sydney, Australia

^b Data 61, CSIRO, Sydney, Australia

ARTICLE INFO

Keywords:

Automated vehicles
Market share
Capacity
Lane dedication
Fundamental diagram

ABSTRACT

Presence of autonomous vehicles (AVs) affects traffic flow characteristics of a mixed traffic stream comprising human-driven vehicles. To model the impact of AVs on the saturation flow of arterials and highways, we propose analytical models to derive the expected value and variance of headway of a traffic stream with mixed AVs and conventional human-driven (or normal) vehicles (NVs), given the *expected* penetration rate of AVs. The proposed model considers the arrangement (order) of AVs and NVs in the mixed stream and the expected, the lowest, and the highest achievable headways and their variability are analytically derived. Moreover, the total delay of a two-lane road with interrupted traffic flow is analytically modeled for various possible lane allocation policies: (a) dedicated lanes, (b) mixed-mixed lanes, (c) mixed-NV lanes, and (d) mixed-AV lanes. Microsimulation experiments demonstrate the validity of the developed models for the average headway and its variability, as well as the delay formulas.

1. Introduction

1.1. Motivation and related literature

The introduction of autonomous vehicles (AVs) is expected to disrupt traffic operations in cities in future. However, an inevitable transition period is envisaged before reaching to a fully automated traffic system. Since AVs have not yet been commercialized and other than a few limited Level 3 and above trials have not been tested on roads, there are numerous aspects that are needed to be scrutinized regarding the impacts of AVs on the traffic flow characteristics of urban and highway roads.

Studies have been carried out to investigate the effects of AVs in combination with conventional human-driven vehicles (or normal vehicles (NVs)) on the road networks (Friedrich, 2016; Talebpour and Mahmassani, 2016; Ghiasi et al., 2017; Chen et al., 2017; Lamotte et al., 2017; Stern et al., 2018; Pan et al., 2019). The main aims of the research in this area are partly to understand the characteristics of the mixed traffic (Arem et al., 2006; Friedrich, 2016; Talebpour and Mahmassani, 2016; Ghiasi et al., 2017; Pan et al., 2019) and partly to propose new algorithms to incorporate the real-time information from connected and automated vehicles (CAV) to improve the efficiency of the traffic network (Ilgin Guler et al., 2014; Argote-Cabañero et al., 2015; Ghiasi et al., 2017; Stern et al., 2018; Hyland and Mahmassani, 2018; Gong and Du, 2018; Tilg et al., 2018).

Arem et al. (2006) studied the effect of vehicles with adaptive cruise control (ACC) and a limited penetration of AVs on the capacity of the mixed traffic, and concluded that under low penetration rates the autonomy may deteriorate the capacity of a

[☆] This article belongs to the Virtual Special Issue on “Traffic flow modeling”.

* Corresponding author.

E-mail address: mohsen.ramezani@sydney.edu.au (M. Ramezani).

<https://doi.org/10.1016/j.trc.2019.10.009>

Received 22 November 2018; Received in revised form 30 August 2019; Accepted 20 October 2019
0968-090X/ © 2019 Elsevier Ltd. All rights reserved.

Nomenclature			
p	Expected penetration rate (EPR) of AVs in the mixed stream	g^ζ	dedicated AV lanes policy that use the mixed lane The green time needed to serve the queued vehicles with the lane capacity in the lane dedicated to vehicles of type $\zeta = \{av, nv, m\}$
nv	Subscript to identify Normal Vehicle	$\mathbb{R}^{m \times n}$	The space of all $m \times n$ real-valued matrices
av	Subscript to identify Autonomous Vehicle	C, R, G, L	Cycle time, red time, green time, and loss time of the controlled approach [sec]
m	Subscript to identify Mixed normal and autonomous vehicles	Q^a	Total arrival flow rate of the traffic [veh/h]
v	Free flow speed of vehicles	$Q^{a,\zeta}$	Arrival flow of vehicles of type $\zeta = \{av, nv, m\}$
n	Total number of vehicles in the mixed traffic stream	$Q^{c,\zeta}$	Saturation flow rate of the traffic of vehicles of type $\zeta = \{av, nv, m\}$ [veh/h/lane]
\bar{h}	Average headway of the mixed traffic stream	K^a	Total density of the arrival traffic [veh/km]
α_{nv}	Proportion of normal vehicles in the mixed-dedicated NV lanes policy that use the mixed lane	$K^{c,\zeta}$	Saturation density of the traffic of vehicles of type $\zeta = \{av, nv, m\}$ [veh/km/lane]
α_{av}	Proportion of autonomous vehicles in the mixed-	$\lfloor \cdot \rfloor$	The floor operator

freeway. Very recently, [Gong and Du \(2018\)](#) proposed a p-step model predictive control algorithm that guarantees the string stability of a platoon of a mixed NV and AV stream with smooth transient response. In the same line of research, [Stern et al. \(2018\)](#) experimentally verified that AVs even under very low penetration rate can be utilized as control actuators to improve the stability of traffic flow on a highway by damping out the stop-and-go waves. The technology of connected vehicles is used in [Han et al. \(2017\)](#) to optimally adjust the speed limit in a variable speed limit motorway. Moreover, [Zhao et al. \(2018\)](#) studied minimizing fuel costs on signalized arterial roads by adjusting the car following behaviour of CAV platoons in a mixed traffic.

Other than controlling AVs in traffic streams, potential governance over lane changing and route choice of CAVs have resulted in numerous applications in improving the efficiency of the future road network ([Yang et al., 2018](#); [Tilg et al., 2018](#); [Yu et al., 2018](#); [Li et al., 2018a](#); [Ramezani and Ye, 2019](#)). For instance, [Tilg et al. \(2018\)](#) proposed a hybrid model to optimize lane changing of CAVs at freeway weaving sections serving a mixed traffic to increase the capacity of bottlenecks. To add, [Li et al. \(2018a\)](#) studied the route choice optimization of CAVs in a network with mixed traffic to maintain the equilibrium or maximize an efficiency measure of the network.

Despite the breadth of valuable knowledge generated on modelling the car-following behavior of CAVs (e.g. [Li and Shrivastava, 2002](#); [Jia and Ngoduy, 2016](#); [Zhou et al., 2017](#); [Sun et al., 2018](#); [Li et al., 2018b](#); [Tuchner and Haddad, 2017](#); [Zhou et al., 2019](#); [Ali et al., 2019](#)), there are a few contributions that study the macroscopic fundamental characteristics of a mixed traffic ([van den Berg and Verhoef, 2016](#); [Chen et al., 2017](#); [Qian et al., 2017](#); [Ghiasi et al., 2017](#)). [van den Berg and Verhoef \(2016\)](#) suggest the capacity of the mixed traffic as a weighted harmonic mean of the capacity of AVs and capacity of NVs. [Chen et al. \(2017\)](#) assuming that all AVs are platooned, derived a mathematical model for the capacity of a mixed platoon and advised the optimal lane allocation policy for a multi-lane road. [Qian et al. \(2017\)](#) by introducing the concept of perceived equivalent density proposed a data-driven macroscopic traffic flow model adapting multiple vehicle classes with known well-defined fundamental diagrams (FD). [Ghiasi et al. \(2017\)](#) proposed an analytical model for the saturation flow of the mixed traffic under arbitrary penetration rate of AVs and a general arrangement of the vehicles in the platoon by adapting a platooning intensity parameter. The model is established based on the assumption of Markovian distribution of AVs, considering a fixed given penetration rate, and stochastic headways between vehicles. They obtained a lower-bound of the actual average saturation flow under the made assumptions.

1.2. Paper's contributions and structure

The main contribution of the paper is to analytically derive macro and steady-state characteristics (i.e. saturation flow and delay) of the mixed traffic flow of AVs and NVs based on micro interactions (i.e. headways) between AVs and NVs. These micro interactions are significantly affected by the penetration rate of AVs and the individual placement of AVs and NVs in the stream. The AV penetration rate is a stochastic variable that changes rapidly over time and over space. Hence, assuming a deterministic or fixed value of AV penetration rate would neglect several realism of the system. The developed analytical models of saturation flow and delay of the mixed traffic take into account the placement (order) of AVs and NVs in the stream and consider the AV penetration rate as a random variable. The models assume the number of AVs in the stream follows the binomial distribution that is stemmed from the nature of the independent arrival of different vehicle types. Note that the AV penetration rate in the paper indicates the percentage of AVs in the traffic stream (platoon of mixed vehicles), rather than the market penetration rate of AVs at the network level that could be a slow-varying variable.

The derived analytical model for the saturation flow of the mixed traffic is used to formulate the total vehicle delay of an interrupted mixed traffic on a two-lane road. Dedication of lanes to different types of vehicles is consequently analyzed and a lane-allocation management strategy is proposed.

In the sequel, the structure of the paper is explained. Section 2 introduces our proposed analytical model to estimate the saturation flow of the mixed traffic. Apart from the general arrangement of vehicles in the traffic investigated in Section 2.1, the worst and best configurations of vehicles resulting in the highest and lowest saturation flows are also studied in Sections 2.2 and 2.3, respectively. Appropriate approximations of the models are presented in Section 2.4, and the models are validated using

microsimulation studies in Section 2.5. Section 3 studies the variability of headways from two perspectives: (1) expected standard deviation (STD) of the average headway because of stochasticity of the AV penetration rate, and (2) the expected STD of the headways within the traffic stream. Section 4 analytically models the total vehicle delay of a two-lane road with a cyclic interrupted flow (e.g. a signalized link), under the four possible lane-allocation policies. The validity of the delay models are verified with microsimulation experiments in Section 4.6. Section 5 proposes a methodology to advise the optimal lane allocation policy for the two-lane road. Finally, Section 6 summarizes the paper and provides the key conclusions and future research directions.

2. Headway analysis of mixed traffic streams

To analyze the traffic flow characteristics of a mixed traffic stream (interchangeably used with traffic platoon), it is essential to obtain the average headway of the mixed stream considering the placement of AVs and NVs in the stream. This is not a trivial task when there is an arbitrary mixture of AVs and NVs in the stream, as the average headway is influenced by headway between normal vehicles (h_{nv-nv}), between AVs (h_{av-av}), between an NV following an AV (h_{av-nv}), and between an AV following an NV (h_{nv-av}). Accordingly in this section, we derive analytical models of the headway of a mixed traffic on a one-lane road given the expected penetration rate of AVs in the stream. It is evident that the individual values of headways between two vehicle types have a direct impact on the traffic flow characteristics of arterial links and freeway segments (Ghiasi et al., 2017). Although the principal headways appear in parametric forms in the developed models, without limiting the generality of the models and for consistency in the results, we assume that AVs have lower headways than NVs, i.e. $[HO] h_{av-av} \leq h_{nv-av} \leq h_{av-nv} \leq h_{nv-nv}$. Unless otherwise stated, for numerical studies we assume $[A] h_{nv-nv} = 1.8$ [sec], $h_{av-av} = 0.9$ [sec], $h_{av-nv} = h_{nv-nv}$, and $h_{nv-av} = h_{av-av} + (h_{nv-nv} - h_{av-av})/3$. The chosen values are in accordance with those reported in the literature (e.g. see Ghiasi et al., 2017).

Accounting for all the possible placement combinations of vehicles in a mixed traffic stream, several arrangements could be considered on a one-lane road. Three arrangements would provide sufficient information to analyze the characteristics of the saturation flow: (i) General arrangement where NVs and AVs are mixed randomly, (ii) the worst arrangement that results in the highest average headway, which is achieved when each AV is followed by an NV depending on the penetration rate, and (iii) the best arrangement that results in the lowest average headway, which is achieved when there is a platoon of AVs in the traffic stream that follows a platoon of NVs. In the following subsections, we derive the headway of the mixed traffic under each of those arrangements.

2.1. General arrangement of AVs in the mixed stream

In the general arrangement of the mixed stream, NVs and AVs are randomly placed in the traffic stream. Due to the nature of the arrival of vehicles, it is conjectured that the number of AVs in the platoon follows a *binomial* distribution. This assumption plays a central role in modelling the average headway of the mixed traffic throughout the paper. Hence, given the Expected Penetration Rate (EPR) of AVs, i.e. $p \geq 0$, the probability of having k AVs in a platoon of n vehicles can be estimated as

$$P(X = k) = C_n^k p^k (1 - p)^{n-k}, \quad C_n^k = \frac{n!}{(n - k)!k!}. \tag{1}$$

Therefore, the expected average headway of a mixed traffic platoon with n vehicles and p as EPR of AVs is:

$$E\left[\bar{h}_k^{\text{general}}(k, n)\right] = \sum_{k=0}^n \bar{h}_k^{\text{general}}(n)P(X = k), \tag{2}$$

$$\bar{h}_k^{\text{general}}(n) = \frac{1}{n - 1} A_k(n)H/C_n^k, \tag{3}$$

where $\bar{h}_k^{\text{general}}(n)$ is the average headway resulting from a stream of n vehicles with k AVs in the stream considering all of the possible combinations. Note that in the definition of $\bar{h}_k^{\text{general}}(k, n)$, $k \in [0, n]$ is a random variable, and $p = E[k/n]$ is the EPR, $H = [h_{nv-nv}, h_{av-av}, h_{nv-av}, h_{av-nv}]^T$, and $A_k(\cdot)$ is the $(k + 1)$ th row of matrix $A(\cdot) \in \mathbb{R}^{(n+1) \times 4}$, which is constructed as (Ramezani et al., 2017):

$$A\left(k + 1, 1\right) = \left(n - 1\right) \left| \sum_{i=0}^k (-1)^i \binom{k + 1 - i}{i} C_n^i \right| \quad k = \{0, \dots, n\}, \tag{4a}$$

$$A(k + 1, 2) = A(k - 1, 1) \quad k = \{2, \dots, n\}, \tag{4b}$$

$$A(k + 1, 3) = A(k + 1, 4) = A(k, 1) \quad k = \{1, \dots, n\}, \tag{4c}$$

$$A(1, 2) = A(1, 3) = A(1, 4) = A(2, 2) = 0. \tag{4d}$$

Matrix A is a function of n . The interpretation of elements of matrix A in row $k + 1$ ($k \in \{0, \dots, n\}$) is that in all the possible arrangements of k AVs in a stream of n vehicles, there are $A(k, 1)h_{nv-nv}$, $A(k, 2)h_{av-av}$, $A(k, 3)h_{nv-av}$, and $A(k, 4)h_{av-nv}$.

It is worth mentioning that matrix $A(\cdot)$ carries a helpful symmetrical property, in a way that $A(k + 1, 1) = A(n - k - 1, 1)$ for $k \geq n/2$ (when n is even) or $k \geq n/2 + 0.5$ (when n is odd). This property is instrumental to avoid large round-off numerical errors in

calculating (4a) for large values of k . Note that the time complexity of (2) grows with n . Therefore, an alternative approximation of (2) is proposed in Section 2.4.

2.2. Worst arrangement (upper-bound headway)

The arrangement of AVs and NVs in the mixed stream that results in the highest possible expected average headway and thus the least (worst) saturation flow, pertains to a configuration that there is no platoon of AVs for $k/n \leq 0.5$, and the leading vehicle is an AV. For higher AV penetrations ($k/n > 0.5$), there will be no platoon of NVs in the traffic stream. Accordingly, the expected worst average headway can be formulated as:

$$E \left[\bar{h}^{\text{worst}}(k, n) \right] = \sum_{k=0}^n \bar{h}_k^{\text{worst}}(n) P(X = k), \tag{5}$$

where

$$\bar{h}_k^{\text{worst}}(n) = \begin{cases} \frac{k \cdot h_{\text{av-nv}} + (k-1)h_{\text{nv-av}} + (n-2k)h_{\text{nv-nv}}}{n-1} & k/n < 0.5 \\ \frac{k \cdot h_{\text{av-nv}} + (k-1)h_{\text{nv-av}}}{n-1} & k/n = 0.5 \\ \frac{(n-k)h_{\text{av-nv}} + (n-k)h_{\text{nv-av}} + (2k-n-1)h_{\text{av-av}}}{n-1} & k/n > 0.5. \end{cases} \tag{6}$$

2.3. Best arrangement (lower-bound headway)

The best arrangement of vehicles, where all AVs are platooned and the leading vehicle is an NV, leads to the lowest possible expected average headway and thus the highest saturation flow. This arrangement is feasible when AVs are connected and there is a controlled lane changing algorithm to facilitate and enforce the formation of the platoon of AVs. The expected average headway with the best arrangement reads:

$$E \left[\bar{h}^{\text{best}}(k, n) \right] = \sum_{k=0}^n \bar{h}_k^{\text{best}}(n) P(X = k), \tag{7}$$

where

$$\bar{h}_k^{\text{best}}(n) = \begin{cases} \frac{(k-1)h_{\text{av-av}} + (n-k-1)h_{\text{nv-nv}} + h_{\text{nv-av}}}{n-1} & 0 < k < n \\ h_{\text{nv-nv}} & k = 0 \\ h_{\text{av-av}} & k = n. \end{cases} \tag{8}$$

2.4. Simplified headway formulas

As the number of vehicles in the platoon, n , increases, Eq. (2) requires larger computational resources. Hence, it is crucial to develop a simplified approximate formula for the expected average headway to make it more applicable to traffic management policies. To this end, fundamental probability theories are sought. We have proved in Proposition 1 in Appendix A that provided Assumption [HO] holds, the headway functions $\bar{h}_k^{\text{general}}(n)$, $\bar{h}_k^{\text{best}}(n)$, and $\bar{h}_k^{\text{worst}}(n)$ are decreasing and concave functions of the AV penetration rate (see Fig. 1(a)). Hence, from Jensen's inequality (Chandler, 1987) the average headway at the expected penetration rate provides an upper-bound for the expected average headway, i.e. $E[\bar{h}^\xi(k, n)] \leq \bar{h}_{\bar{k}}^\xi$, where $\xi = \{\text{general, worst, best}\}$, and $\bar{k} = E[k] = \lfloor np \rfloor$.

As such, one can approximate the expected average headway for each arrangement as the average headway with \bar{k} AVs in the platoon, i.e.

$$E[\bar{h}^\xi(k, n)] \approx \bar{h}_{\bar{k}}^\xi |_{\bar{k}=\lfloor np \rfloor}. \quad \xi = \{\text{general, worst, best}\} \tag{9}$$

Upper-bounds of the errors due to this approximation (also called Jensen's gap) are provided in Proposition 2 in Appendix A. Fig. 1(a) confirms the high accuracy of (9) in estimating the expected average headways.

Further scrutinizing the expected headway formula (2), it can be written as a function of the principal headways h_{i-j} , $i, j \in \{\text{nv, av}\}$ as follows:

$$E[\bar{h}(k, n)] = \gamma_{\text{nv-nv}}(p, n)h_{\text{nv-nv}} + \gamma_{\text{av-av}}(p, n)h_{\text{av-av}} + \gamma_{\text{nv-av}}(p, n)h_{\text{nv-av}} + \gamma_{\text{av-nv}}(p, n)h_{\text{av-nv}}, \tag{10}$$

where $0 \leq \gamma_{i-j}(p, n) \leq 1$, $i, j \in \{\text{nv, av}\}$, are the resulting coefficients that are functions of number of vehicles in the platoon, n , and the EPR, p . Sketching the coefficients of headways $\gamma_{i-j}(p, n)$ with respect to p in Fig. 2(a), highlights that $\gamma_{\text{nv-av}}$ and $\gamma_{\text{av-nv}}$ are almost equal for each considered arrangement, and their lowest and highest values belong to the best and worst arrangements, respectively. Moreover, it is observed from the figure that coefficients $\gamma_{i-j}(p, n)$ for the general arrangement are closer to their corresponding values for the worst arrangement at various p . Therefore, the mixed traffic in general behaves more closely to the worst arrangement,

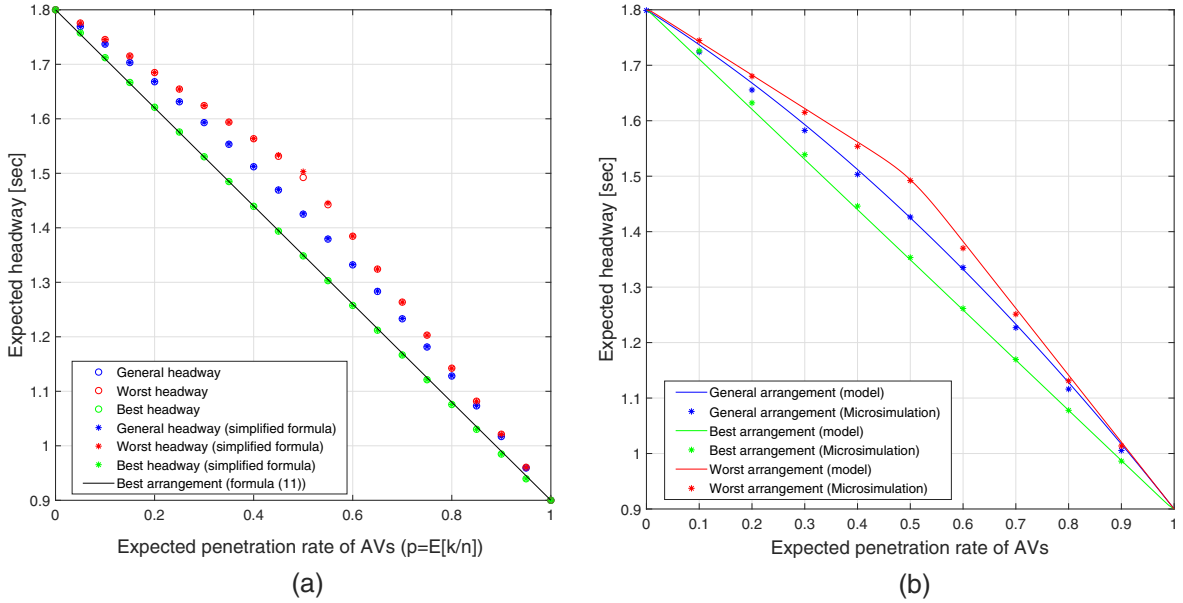


Fig. 1. (a) The expected average headways obtained from the accurate and approximate formulas for the same traffic stream taking various EPRs of AVs (p). It is clear that the headways acquired from the accurate and approximate formulas are compliant. The expected average headways obtained from (11) are also plotted for comparison. (b) Comparison of the expected average headway obtained from microsimulation and the proposed model for various expected AV penetration rates and the general, best, and worst arrangements.

and approximating the average headway by the best arrangement could intrinsically result in the overestimation of the saturation flow, unless the technology facilitates platooning of AVs.

Moreover, it is clear from Fig. 2(a) that for the best arrangement $\gamma_{av-nv} = 0$, $\gamma_{nv-av} \approx 0$, $\gamma_{av-av} \approx p$, and $\gamma_{nv-nv} \approx 1 - p$, suggesting the following alternative formula that was also proposed in Friedrich (2016):

$$E[\bar{h}^{best}(p, n)] \approx ph_{av-av} + (1 - p)h_{nv-nv}. \tag{11}$$

Model (11) is indeed an approximation of (9) when n is large enough (i.e. $n \rightarrow \infty$). Moreover, given the expected values of the headway components, other simplified models can be established for the expected average headway under various vehicle arrangements using a linear regression over the calculated values from the more detailed models. For instance, given the values in Assumption [A], the expected average headway under the general arrangement can be accurately estimated as

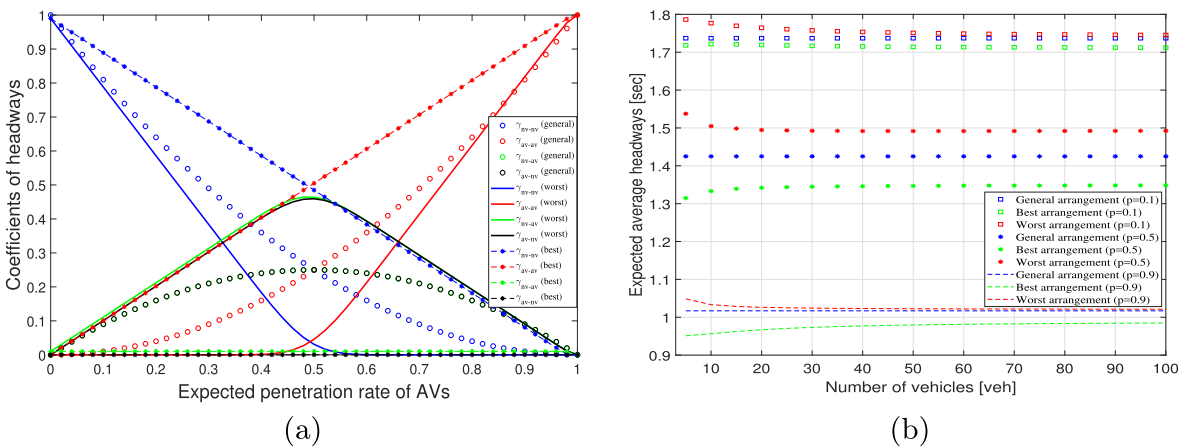


Fig. 2. (a) Coefficients of headway terms γ_{i-j} ($i, j = \{av, nv\}$) in (10) as functions of the EPR for a stream of 100 vehicles under various platoon configurations: (i) the general arrangement (2), (ii) the worst arrangement (the highest headway) (5), and (iii) the best arrangement (the lowest headway) (7). Note that the highest influence of coefficients γ_{nv-av} and γ_{av-nv} is on the expected average headway of the worst arrangement, and their lowest influence is on the best arrangement. (b) Variations of the expected average headways obtained from the proposed models with respect to the number of vehicles in the traffic stream under three different expected AV penetration rates of 10%, 50%, and 90%. General, worst, and best vehicle arrangements are investigated.

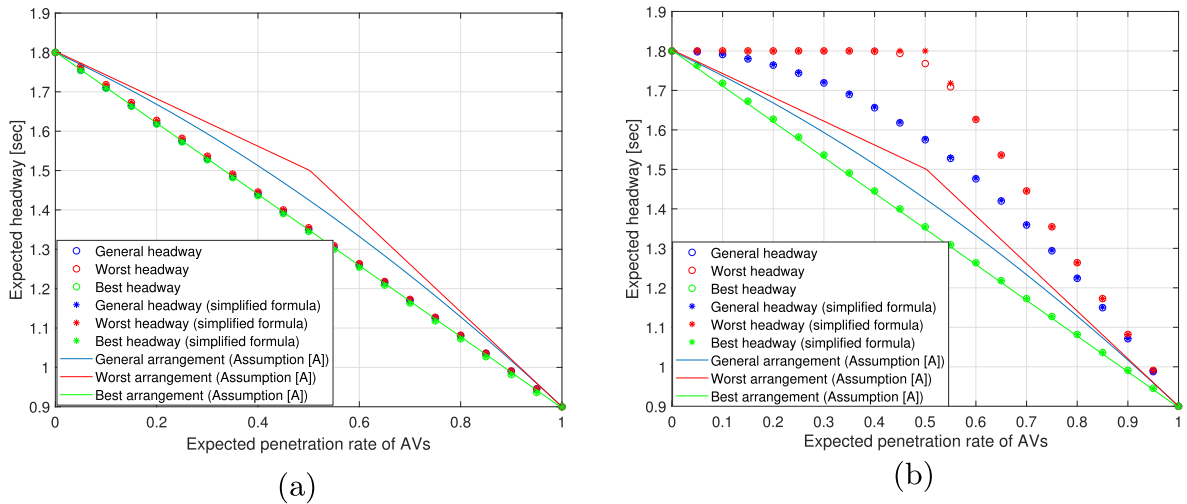


Fig. 3. The effect of changing headway components on the expected average headways via changing h_{av-nv} in Assumption [A]. The expected average headways are obtained from the accurate and approximate formulas for a mixed platoon of $n = 100$ vehicles taking various EPRs of AVs, p . (a) $h_{nv-nv} = h_{av-nv} = 1.8$ [sec] and $h_{av-av} = h_{nv-av} = 0.9$ [sec], and (b) $h_{nv-nv} = h_{av-nv} = h_{nv-av} = 1.8$ [sec], $h_{av-av} = 0.9$ [sec]. The headways resulted from dictating Assumption [A] are depicted by solid lines for comparison.

$$E[\bar{h}(k, n)] \approx -0.3p^2 - 0.6p + 1.8, \text{ where } p = E[k/n] \text{ (Ramezani et al., 2017).}$$

Remark 1. Although models (2), (5), and (7) relate the expected average headway as a function of the number of vehicles in the platoon (n), further investigation of the headway formulas demonstrated in Fig. 2(b) reveals that the effect of n is not significant. Fig. 2(b) shows that the average headway of the general arrangement is indifferent to the number of vehicles, and the headways of the best and worst arrangements remain unchanged for $n > 35$ [veh] and slightly vary with lower values of n .

Remark 2. Other than the difference between h_{av-av} and h_{nv-nv} , the values of h_{av-nv} and h_{nv-av} have a significant effect on the average headway difference between the best and worst arrangements. For clarification, we have studied the effect of changing Assumption [A] in Fig. 3 by studying two extreme cases for h_{nv-av} : (a) $h_{nv-av} = h_{av-av}$ and (b) $h_{nv-av} = h_{nv-nv}$. The results indicate that in Case (a) the highest average headway difference between the best and worst arrangements has reduced to 0.005 [sec] from 0.2 [sec], whereas in Case (b) the difference has significantly increased to 0.42 [sec]. Note that the results of the best arrangement has remained the same, highlighting that this particular arrangement may not capture the interaction of different vehicle types in random arrangements of vehicles in the platoon.

2.5. Validation of the expected average headway models using microsimulation

The proposed macro and steady-state models for the expected average headway are derived by assuming deterministic headways between vehicles types and neglecting micro dynamics of vehicles such as acceleration and deceleration. To validate the modelled headway formulas (2), (5) and (7), microsimulation experiments (in Aimsun) were conducted. Each arrangement was implemented on a one-lane road. The capacity (inverse of the headway) of the mixed flow was measured using a virtual loop detector located at the downstream of the road in the steady-state condition. Headway characteristics of NVs and AVs following an AV or NV were enforced through the Aimsun application programming interface (API).

Note that although the modelled average headway formulas consider the variability of penetration rate of AVs, they do not take the variability of individual headway terms h_{i-j} ($i, j \in \{av, nv\}$) into consideration. However, a microsimulation test-bed provides the opportunity to also take this variability into effect, and investigate possible arising errors due to neglecting this factor. Microsimulation results in Fig. 1(c) fully affirm the validity of the proposed models adopting different expected penetration rates. The results of this comparative study are important from two aspects: (i) they show that the binomial distribution of the number of AVs in the platoon of mixed traffic is a valid assumption, and (ii) slight variability of headway terms h_{i-j} do not have a considerable impact on the expected average saturation flow of the mixed traffic.

3. Expected Standard Deviation (STD) of headways

String stability of a platoon is defined as the ability of the car-following behaviour of the vehicles to attenuate small perturbations in the equilibrium headway of vehicles created in the downstream of the platoon (Talebpoor and Mahmassani, 2016; Sun et al., 2018). Within a heterogeneous traffic flow, the headways between vehicles are not fixed. Hence, the variability of headways in a mixed traffic plays an important role in characterizing the string stability. The variability of headways can be looked at from two perspectives: (1) the variability of the average headway of the traffic due to the stochasticity of the penetration rate, and (2) the

average variability among the set of headways within the stream. The former can be straightforwardly estimated from (2), (5), and (7) following the definition:

$$\text{Var} \left[\bar{h}^\zeta(p, n) \right] = \sum_{k=0}^n (\bar{h}_k^\zeta(n) - E[\bar{h}^\zeta(p, n)])^2 P(X = k), \tag{12}$$

where $\zeta = \{\text{general, worst, best}\}$.

To accurately estimate the headway variability of the traffic stream in the general arrangement, one should generate all the possible traffic streams given k AVs among total of n vehicles, i.e. C_n^k different combinations of the stream. This reads as:

$$E \left[\overline{STD}^{\text{general}}(p, n) \right] = \sum_{k=0}^n \overline{STD}_k^{\text{general}}(n) P(X = k), \tag{13}$$

with

$$\overline{STD}_k^{\text{general}}(n) = \frac{1}{C_n^k} \sum_{i=1}^{C_n^k} \sqrt{\frac{\sum_{j=1}^{n-1} (h_{i,j} - \bar{h}_{k,i}^{\text{general}}(n))^2}{n-1}}, \tag{14}$$

where $h_{i,j}$ is the j th headway in the i th traffic stream combination ($j \in \{1, \dots, n-1\}; i \in \{1, \dots, C_n^k\}$), and $\bar{h}_{k,i}^{\text{general}}(n)$ is the average headway of stream i with k AVs. The RHS of Eq. (14) averages the standards deviation of the set comprising individual headways in each traffic stream combination.

For each of the worst and best arrangements, a single configuration is conjectured given the number of AVs in the platoon. As such, for $\xi = \{\text{worst, best}\}$ we have:

$$E \left[\overline{STD}^\xi(p, n) \right] = \sum_{k=0}^n \overline{STD}_k^\xi(n) P(X = k), \tag{15}$$

where

$$\overline{STD}_k^\xi(n) = \sqrt{\frac{\sum_{j=1}^{n-1} (h_j - \bar{h}_k^\xi(n))^2}{n-1}}, \tag{16}$$

h_j is the j th headway in the traffic stream, and $\bar{h}_k^\xi(n)$ is the average headway of the stream with k AVs.

Fig. 4(a) depicts the STD of the expected headway of the mixed traffic as a result of the uncertainties in the penetration rate, where the maximum variability occurs at $p = 0.64$ for the general arrangement, $p = 0.67$ for the worst arrangement, and $p = 0.5$ for the best arrangement of vehicles. Moreover, it is shown in Fig. 4(b) that the variation of the expected STD of the stream’s headway for various AV penetration rates (demonstrated in (14)) is independent of the number of vehicles in the traffic stream. To add, Fig. 4(c) sketches the expected STD of a stream of 20 vehicles for various EPRs and different arrangements. According to the figure, the headways have the most variability at $p = 0.6$ for the general arrangement, $p = 0.5$ for the best arrangement, and $p = 0.7$ for the worst arrangement.

The analytical models (13) and (15) are compared against microsimulation results in Fig. 4(c). Three sources contribute to the variability of traffic’s headway in the microsimulation: (i) the configuration in the platoon, (ii) uncertainty of AVs’ penetration rate, and (iii) stochasticity of each headway component $h_{i-j}, i, j \in \{nv, av\}$. The first two sources are captured in our models (13) and (15), whereas the third source is neglected. Accordingly, we observe considerable variability of headways under 100% penetrations of AVs

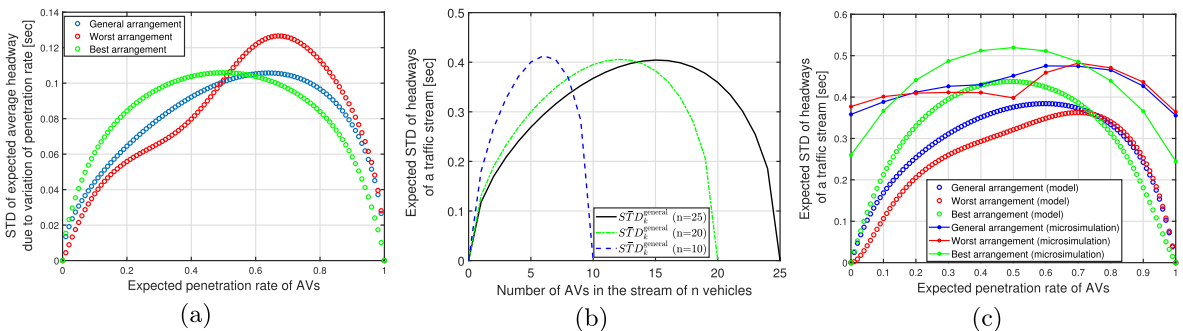


Fig. 4. (a) The STD of the average headway of a traffic stream comprising 20 vehicles, obtained from (12) for different EPRs and undertaking various studied arrangements. (b) Expected STD of headways for a stream of $n = \{10, 20, 25\}$ vehicles with different number of AVs under the general arrangement, obtained from (14). (c) The expected STD of headways of a traffic stream comprising 20 vehicles, and their comparison with the expected STD of headways of a traffic stream obtained from microsimulation experiments adapting various EPRs and different vehicle arrangements.

or NVs in the microsimulation, which are not foreseen by the analytical models. This explains a bias that is apparent between the theoretical models and the microsimulation results. Nevertheless, it is observed that the microsimulation and the models returned the same EPRs at which the STD of stream’s headway is maximum. In other words, the modelled STD of stream’s headway can capture the critical values of the real trend for the general, worst and, best arrangements.

4. Delay analysis of interrupted mixed traffic in a two-lane road

Total vehicle delay of interrupted traffic flow (e.g. experienced by vehicles in the queue because of traffic signals), is a crucial criterion to measure the efficiency of traffic control plans on urban links. In this section, based on the headway analysis in Section 2 and without the loss of generality, we formulate the delay of an interrupted mixed traffic flow in a two-lane link considering four possible lane-allocation policies: (i) Dedicated lanes (AV lane - NV lane), (ii) Mixed lane - mixed lane, (iii) Mixed lane - NV lane, and (iv) Mixed lane - AV lane. This formulation is essential to devise the optimal lane allocation management method to decrease the total delay of mixed traffic considering the effect of traffic signals. The proposed formulations can be extended to a multi-lane approach as a future research direction.

To derive the analytical formulations, as in Mohajerpoor et al. (2019) we assume: [H1] infinite acceleration and deceleration; [H2] the arrival flow and free flow speed of the approach are constant and known during the cycle time; [H3] a triangular fundamental diagram; [H4] the loss-time of the approach is known and constant, and [H5] the introduction of AVs does not change the jam density of the mixed traffic. Note that we validate the analytical delay models with microsimulation experiments to scrutinize the effect of above assumptions in Section 4.6.

Let us denote the signal cycle length and the green time, red time, and loss time of the approach by C , G , R , and L , respectively. It is evident that $C = R + L + G$. The number of arrived vehicles to the approach during a cycle is $n_a = \lfloor Q^a C \rfloor$, where Q^a is the arrival flow of the mixed traffic at the controlled approach. Note that due to different reaction times of NVs and AVs, loss-time of each lane could be different. In light of that, we define $L = \max\{L_{\zeta_1}, L_{\zeta_2}\}$, where L_{ζ_i} is the loss-time of lane idedicated to type $\zeta_i \in \{nv, av, m\}$. The proposed delay models are derived for one cycle time. As such, they can be directly employed for the sake of adaptive cycle-by-cycle signal optimization and lane management. Note that we assume the arrival flows under each lane-dedication policy are bounded in a way that the approach remains *undersaturated*. For example, when the dedicated lanes policy is employed, and the AV penetration rate is 0%, the arrival flow rate at the approach should be less than $(3600/h_{nv-nv})G/C$.

4.1. Dedicated lanes policy

This lane allocation policy dedicates one lane to AVs and one lane to NVs. We assume the number of AVs arriving during a cycle is a random variable with a binomial distribution. Consequently, the expected total delay of vehicles under this policy and assuming p is the EPR of AVs is

$$E \left[D^{nv-av} \left(k, n_a \right) \right] = \sum_{k=0}^{n_a} D_k^{nv-av} P \left(X = k \right), \tag{17}$$

where

$$D_k^{nv-av} = \sum_{\zeta=av, nv} \frac{0.5Q_k^{a,\zeta} K_k^{c,\zeta}}{K_k^{c,\zeta} - K_k^{a,\zeta}} (R + L_{\zeta})^2, \tag{18}$$

and k is the number of AVs arrived during the cycle. Moreover, $Q_k^{a,av} = \frac{k}{n_a} Q^a$, $Q_k^{a,nv} = \left(1 - \frac{k}{n_a}\right) Q^a$, D_k^{nv-av} , $K_k^{a,\zeta}$, and $K_k^{c,\zeta}$ respectively denote the arrival flow of AVs, the arrival flow of NVs, the total vehicle delay of the approach, and the arrival and saturation densities for vehicles of type $\zeta = \{av, nv\}$, given k AVs arrived during the cycle. Notably, independent from the penetration rate k/n_a , the saturation flow for the dedicated lanes are $Q_k^{c,av} = Q^{c,av} = 3600/h_{av-av}$ and $Q_k^{c,nv} = Q^{c,nv} = 3600/h_{nv-nv}$. Assuming stationary uncongested arrival traffic state and Assumption [H3], the arrival and saturation densities can be calculated given the free flow speed of the arrival traffic, V , as $K_k^{a,\zeta} = Q_k^{a,\zeta}/V$ and $K_k^{c,\zeta} = Q_k^{c,\zeta}/V$, respectively ($\zeta = \{av, nv, m\}$).

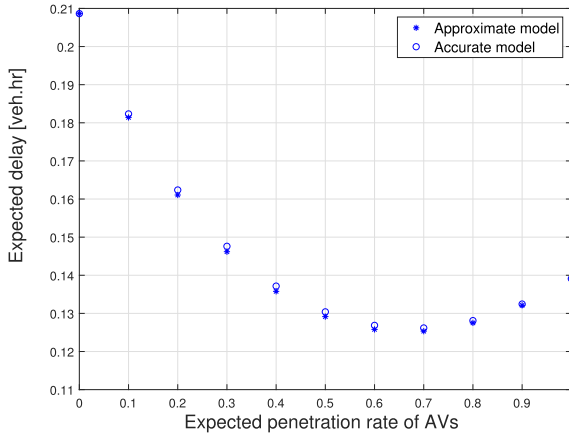
To investigate the effect of EPR on the expected delay of the approach, the delay is plotted against various EPRs in Fig. 5(a) for a signalized approach with $C = 120$ [sec], $R = 50$ [sec], and $L = 2$ [sec], where the traffic fulfills Assumption [A], together with the following traffic flow characteristics:

Assumption [B]: $Q^a = 1000$ [veh/h] and $V = 60$ [km/h].

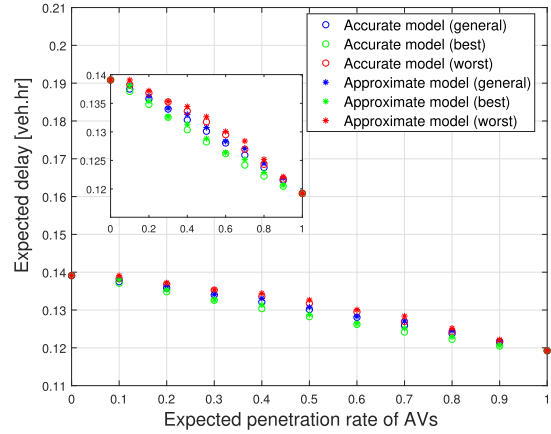
Fig. 5(a) shows that the expected delay $E[D^{nv-av}(k, n_a)]$ is a convex function of the EPR, where its minimum occurs at $p = 0.7$. That is the dedicated lanes policy is beneficial in improving the traffic flow at relatively high market share of AVs around 70%. It is clear that under higher penetration of AVs, the dedicated lane for NVs would be under-utilized, which itself increases the overall delay of the approach.

4.2. Mixed-mixed lanes policy

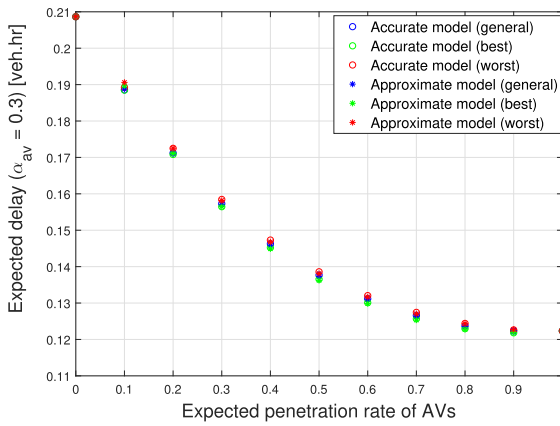
AVs and NVs could use both lanes with the mixed-mixed lanes policy. Assuming under this policy, the distribution of AVs (and also NVs) between the two lanes follows an equilibrium condition (e.g. equal queueing delay for both lanes), the expected total delay



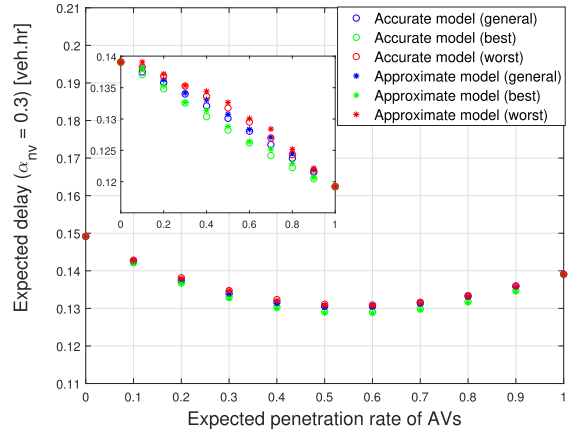
(a) Dedicated lanes



(b) Mixed-mixed lanes



(c) Mixed-AV lanes



(d) Mixed-NV lanes

Fig. 5. Expected total vehicle delays of a two-lane approach adopting various lane management policies during a cycle for various EPRs. The results are obtained from the accurate and approximate models. Total arrival flows of the approach is $Q^a = 1000$ [veh/h], cycle time is $C = 120$ [sec], loss-time is $L = 2$ [sec], and red time is $R = 50$ [sec]. (For interpretation of the references to color in this figure legend, the reader is referred to the web version of this article.)

of vehicles is

$$E \left[D^{m-m} \left(k, n_a \right) \right] = 2 \sum_{k=0}^{n_a} D_k^{m-m} P \left(X = k \right), \quad (19)$$

where

$$D_k^{m-m} = \frac{0.5Q^{a,m}K_k^{c,m}}{K_k^{c,m} - K^{a,m}} (R + L)^2. \quad (20)$$

$Q^{a,m}$ and $K^{a,m}$ are the arrival flow and density of each mixed lane, respectively. Note that it is not necessary for the flow of both mixed lanes neither to be equal, nor equal proportions of AVs to occupy each lane. However, under equilibrium queueing delay condition that is intrinsically applied by road users, we may safely make those assumptions in the aggregate level. Therefore, we assume that $Q^{a,m} = 0.5Q^a$ and $K^{a,m} = 0.5K^a$. Moreover, using (3), the saturation flow of each lane is

$$Q_k^{c,m} = \frac{3600}{\bar{h}_k^{m-m}}, \quad (21)$$

where $\bar{h}_k^{m-m} = \frac{1}{n_a - 1} A_k(n_a) H / C_{n_a}^k$ for the general arrangement of vehicles. For the worst and best arrangement of vehicles in the mixed lanes, the average headway in (21) should be replaced by \bar{h}_k^{worst} and \bar{h}_k^{best} defined in (6) and (8) for $n = n_a$, respectively. Fig. 5(b) plots the expected total delay of the approach for various EPRs undertaking the traffic conditions specified in Assumptions

[A] and [B]. It can be seen that the expected delay under the arbitrary arrangement of vehicles is a decreasing function of the EPR. That is, increase in market share of AVs improves the traffic delay under the mixed-mixed lanes policy.

4.3. Mixed-AV lanes policy

Under the mixed-AV lanes policy, one lane is dedicated to AVs and the other lane is allocated to both AVs and NVs. To model the delay, it is crucial to explicitly consider the proportion of AVs using the mixed lane, denoted as $\alpha_{av} \in [0, 1]$. Obtaining the optimum value of α_{av} (for minimizing the total delay or user-equilibrium delay) is addressed in Section 5.1. Assuming k arriving AVs during the cycle, the arrival flow of each lane is $Q_k^{a,m} = \alpha_{av} \frac{k}{n_a} Q^a + \left(1 - \frac{k}{n_a}\right) Q^a$, and $Q_k^{a,av} = \left(1 - \alpha_{av}\right) \frac{k}{n_a} Q^a$. The saturation flow for the AV lane is obtained from Section 4.1, and for the mixed lane it reads as $Q_k^{c,m} = \frac{3600}{\bar{h}_k^{m-av}(\alpha_{av})}$, with $\bar{h}_k^{m-av}(\alpha_{av}) = \frac{1}{n_{a2}-1} A k_2 (n_{a2}) H / C_{n_{a2}}^{k_2}$, $n_{a2} = n_a - k + k_2$, and $k_2 = \lfloor \alpha_{av} k \rfloor$. Accordingly, the expected total vehicle delay of the approach can be formulated as:

$$E \left[D^{m-av} \left(k, n_a, \alpha_{av} \right) \right] = \sum_{k=0}^{n_a} D_k^{m-av} P \left(X = k \right), \tag{22}$$

where

$$D_k^{m-av} = \sum_{\zeta=m,av} \frac{0.5 Q_k^{a,\zeta} K_k^{c,\zeta}}{K_k^{c,\zeta} - K_k^{a,\zeta}} (R + L_\zeta)^2. \tag{23}$$

Assuming $\alpha_{av} = 0.3$ and traffic conditions defined in Assumptions [A] and [B], Fig. 5(c) demonstrates the expected total vehicle delay of the approach for various EPRs and the general, best, and worst arrangements of vehicles in the mixed lane. It can be seen that the delay is a decreasing and convex function of the EPR, i.e. this policy is more effective as the market share of AVs grows. Note that fixing 30% of AVs to occupy the mixed lane (i.e. $\alpha_{av} = 0.3$) is not optimum for the entire EPR range, and employing the user-delay equilibrium or system-delay optimum values introduced in Section 5.1 is advised in calculating (22).

4.4. Mixed-NV lanes policy

The Mixed-NV lanes policy dedicates a lane to NVs and allocates the other lane to both AVs and NVs. Similar to the mixed-AV lanes policy, it is crucial to estimate the proportion of NVs that use the mixed lane. The proportion, denoted as $\alpha_{nv} \in [0, 1]$, can be optimized to minimize the total delay or represent user-delay equilibrium. This problem is addressed in Section 5.1. As such, assuming k AVs arriving during the cycle, the arrival flow rate for mixed and NV lanes are $Q_k^{a,m} = \frac{k}{n_a} Q^a + \alpha_{nv} \left(1 - \frac{k}{n_a}\right) Q^a$ and $Q_k^{a,nv} = \left(1 - \alpha_{nv}\right) \left(1 - \frac{k}{n_a}\right) Q^a$, respectively. To add, the saturation flow for the mixed lane under the general arrangement of vehicles is approximated as $Q_k^{c,m} = \frac{3600}{\bar{h}_k^{m-nv}(\alpha_{nv})}$, where $\bar{h}_k^{m-nv}(\alpha_{nv}) = \frac{1}{n_{a1}-1} A k (n_{a1}) H / C_{n_{a1}}^k$, and $n_{a1} = k + \lfloor \alpha_{nv} (n_a - k) \rfloor$. Accordingly, the average headway for the mixed lane under the best and worst arrangements can be obtained from (8) and (6) for $n = n_{a1}$, respectively.

The expected vehicle delay for the approach can thus be written as

$$E \left[D^{m-nv} \left(k, n_a, \alpha_{nv} \right) \right] = \sum_{k=0}^{n_a} D_k^{m-nv} P \left(X = k \right), \tag{24}$$

where

$$D_k^{m-nv} = \sum_{\zeta=m,nv} \frac{0.5 Q_k^{a,\zeta} K_k^{c,\zeta}}{K_k^{c,\zeta} - K_k^{a,\zeta}} (R + L_\zeta)^2. \tag{25}$$

Fig. 5(d) shows the total expected delay of the approach assuming $\alpha_{nv} = 0.3$ and the traffic characteristics defined in Assumptions [A] and [B] for various EPRs and different arrangements of vehicles in the mixed lane. Given that always 30% of NVs use the mixed lane, the minimum delay occurs at $p = 0.55$ for various arrangements of vehicles. Moreover, platooning of AVs has shown to be effective in reducing the delay of the approach, particularly for expected AV penetration rates between 0.4 and 0.8. Note that $\alpha_{nv} = 0.3$ is not optimal for every EPR (see Fig. 7), and it is advised to use either the user-delay equilibrium or the system-delay optimum value of α_{nv} when calculating the total delay (see Section 5.1).

4.5. Simplified delay formulas

Obtaining simplified formulas for the total delay models is essential, particularly when there are a large number of vehicles arriving in one cycle, multiple approaches at the intersection, and multiple intersections' signals to be optimized simultaneously. In these situations, significant numerical complexities could be invoked by formulas (17), (19), (24), and (22) into the signal

optimization program. Similar to headway models, the expected delay model for each policy $\zeta = \{nv - av, m - m, m - nv, m - av\}$ can be approximated as the delay at the expected AV penetration rate, i.e. for $\bar{k} = \lfloor n_a p \rfloor$:

$$E[D^{nv-av}(k, n_a)] \approx D_{\bar{k}}^{nv-av} \quad (26a)$$

$$E[D^{m-m}(k, n_a)] \approx D_{\bar{k}}^{m-m} \quad (26b)$$

$$E[D^{m-av}(k, \alpha_{av}, n_a)] \approx D_{\bar{k}}^{m-av}(\alpha_{av}) \quad (26c)$$

$$E[D^{m-nv}(k, \alpha_{nv}, n_a)] \approx D_{\bar{k}}^{m-nv}(\alpha_{nv}) \quad (26d)$$

The errors due to this approximation are essentially bounded, and an upper-bound for the Jensen's gap for each policy is provided in Proposition 3 in Appendix A. The validity of formulas (26a), (26b), (26c), and (26d) are numerically examined in Figs. 5(a), (b), (c), and (d), respectively, wherein the delays obtained from the accurate and approximate formulas are compared for various EPRs. The results affirm that the approximate formulas have acceptable accuracy in estimating the expected total delay of the approach, with often less than 1% estimation errors.

4.6. Validation of the delay models using microsimulation experiments

This section presents the microsimulation results conducted to evaluate the validity of the proposed analytical expected total delay models. The evaluation is valuable due to the possible effects stemming from the following assumptions (or simplifications) made to develop the delay models: [I] the stochasticity of the headway components (h_{ij}) is ignored; [II] Assumptions [H1] to [H5]; [III] under the mixed-mixed lane policy AVs are equally distributed between the lanes; [IV] the lane changing behavior of traffic which influences the values of α_{nv} and α_{av} in the mixed-NV and mixed-AV delay models is not considered; and [V] the delay of each lane is approximated by the kinematic wave model (Mohajerpoor et al., 2017). Note that the saturation flow models have been formerly validated via microsimulation experiments in Section 2.5.

We conducted microsimulation studies (10 replications of a 1-h experiment) on a hypothetical intersection, and measured the total vehicle delay at a two-lane approach for various EPRs and different lane management policies. The traffic of the approach complied with Assumptions [A] and [B] with $C = 120$ [sec], $R = 42$ [sec], and $L = 1.1$ [sec]. The mixed lanes adopted the general (stochastic) arrangement of vehicles. Note that the microsimulation model does not exhibit the above-mentioned simplifications [I-V] to replicate the dynamics of the traffic.

The results of the microsimulation experiments and their comparison with the proposed delay models are depicted in Fig. 6 for various EPRs and different lane allocation policies. The proportions α_{ζ} ($\zeta = \{nv, av\}$) for the mixed-dedicated lanes policies are selected from the following criteria: (i) the average of measured values obtained from the microsimulation experiments, and (ii) the optimal values α_{ζ}^{opt} attained from minimizing the delay (see Section 5.1 for further details). Moreover, the figure shows the percentage errors of the modelled values of delays with respect to the ground truth (microsimulation results), for various EPRs and different lane management policies.

According to Fig. 6, despite Assumptions [I-V], the proposed delay models agreeably lead to accurate estimations, supported by the microsimulation results for each studied policy. Closer look at the accuracy of the modelled delays, further indicates that the modelled values carry errors of less than 3% for the mixed-mixed and mixed-dedicated lanes policies, and less than 8% for the dedicated lanes policy. The modelled delay for the dedicated lanes policy slightly underestimates the delays from microsimulation for EPRs between 0.7 and 0.9. In addition, Fig. 6 (c-d) demonstrate the effectiveness of enforcing the optimal proportions of NVs and AVs to use their dedicated lanes in the mixed-NV and mixed-AV lanes policies to reduce the total delay of the approach. This is investigated in Section 5.1.

5. Real-time optimal lane management of a two-lane road

The aim of this section is to design an algorithm to choose the best policy for a two-lane arterial road with a mixed AV and NV traffic and p as an expected penetration rate of AVs. In light of that, the objective is minimizing the total delay. The lane management policy can be updated in real-time depending on the variation of the expected AV penetration rate. However, we assume p remains unaltered for a certain time duration, which is denoted T hereafter.

5.1. Optimization of α_{av} and α_{nv}

As previously discussed, in the mixed-dedicated lane allocation policy, parameters α_{av} and α_{nv} , i.e. respectively the ratio of AVs and NVs that use the mixed lane, directly influence the arrival flow rates, the headway (thus saturation flow) of the mixed lane, and consequently the total delay. Therefore, choosing appropriate values for α_{ξ} , $\xi = \{av, nv\}$, given the expected AV penetration rate is crucial. In this section two alternative methods are studied to optimize α_{ξ} given the EPR for the $m - \xi$ policy: (i) satisfying the queueing-delay equilibrium (or user-delay equilibrium) condition, and (ii) minimizing the total delay. The former criterion is based on the assumption that the steady-state traffic inherently satisfies the following equilibrium condition:

$$\frac{Q^{a,m}}{Q^{c,m}} = \frac{Q^{a,\xi}}{Q^{c,\xi}} \quad \xi = \{nv, av\}. \tag{27}$$

Condition (27) implies that the ratio of the arrival and saturation flows of the lanes are equal in the steady-state that is the queue size (and consequently the queueing delay) of both lanes are equal. The saturation flow of the mixed lane is itself a function of the proportion α_ξ , as the number of AVs (NVs) in the mixed-AV (mixed-NV) policy that use the mixed lane influences the AV penetration rate at the mixed lane. Moreover, as shown in Section 2.4 the expected headway of the general (stochastic) arrangement of vehicles can be well approximated by a second order polynomial function of the EPR, $E[\bar{h}(k, n)] = b_2 p^2 + b_1 p + b_0$. As such, the following formula based on (27) governs the User-delay Equilibrium (UE) proportions of vehicles using the mixed lane α_ξ^{UE} :

$$a_{\zeta 2}(\alpha_\xi^{UE})^2 + a_{\zeta 1}\alpha_\xi^{UE} + a_{\zeta 0} = 0 \quad \zeta = \{nv, av\}, \tag{28}$$

where $a_{\zeta i}$, $i = \{0, 1, 2\}$, which are functions of the EPR (p), headways $h_{\zeta-\xi}$, and b_0 , b_1 , and b_2 , are defined in Appendix B. It is clear that the admissible solution of (28) should satisfy $0 \leq \alpha_\xi^{UE} \leq 1$.

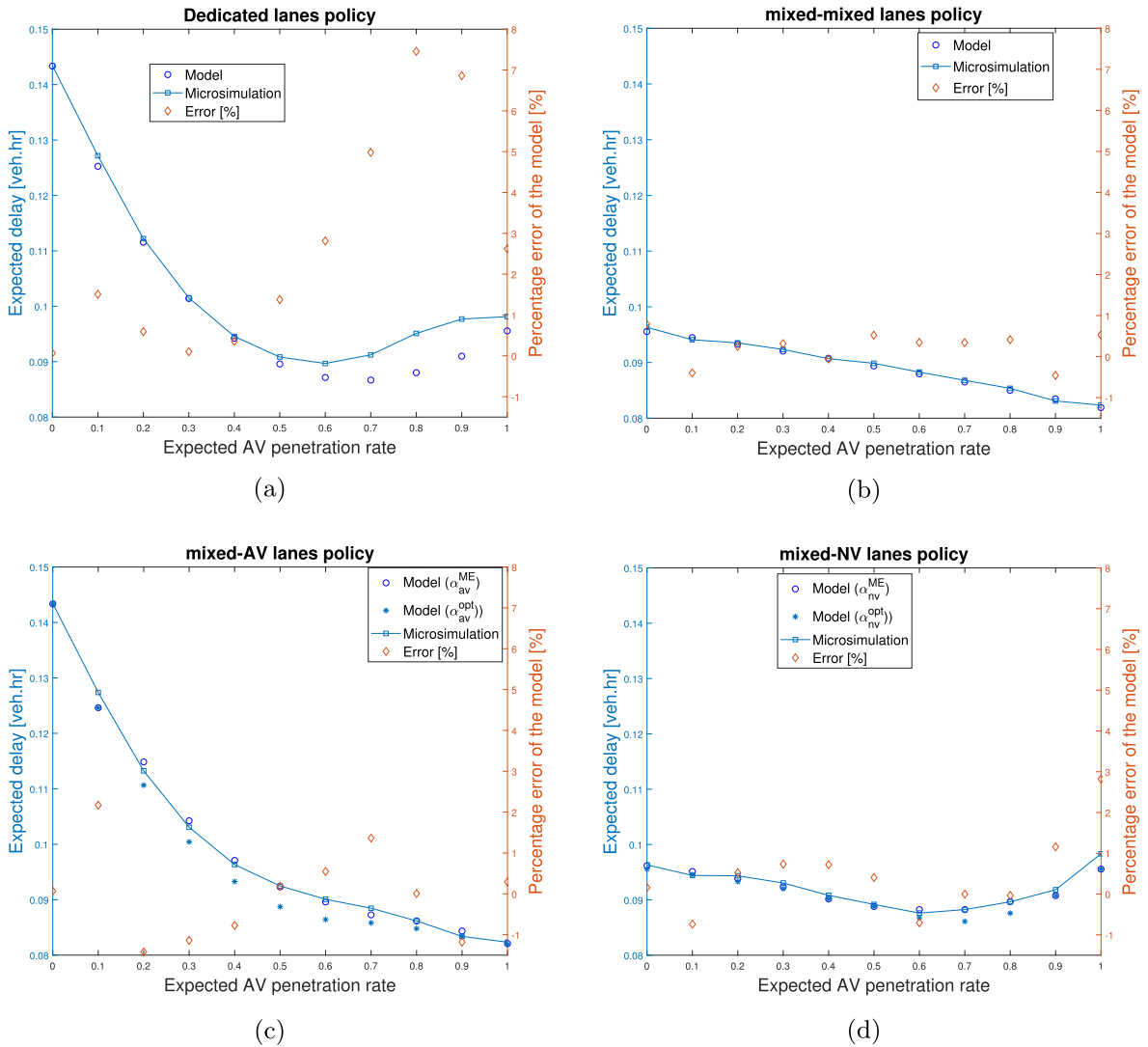


Fig. 6. Comparison of the expected total vehicle delays obtained from the proposed models and microsimulation studies for various EPRs and different lane management policies, conducted on a two-lane approach complying with Assumptions [A] and [B] with $C = 120$ [sec], $R = 42$ [sec], and $L = 1.1$ [sec]. In addition, the percentage errors of the modelled delays for various EPRs and each lane management policy (with respect to the microsimulation results) are depicted in each sub-figure as the second y-axis. The proportions α_ξ ($\xi = \{nv, av\}$) in the mixed-dedicated lanes policies (i.e. sub-figures (c,d)) adopt two sets of values: (i) the measured microsimulation equilibrium (ME) values obtained from the experiments (α_ξ^{ME}) and (ii) the optimum α_ξ^{opt} obtained from (O1), which minimizes the delay of the approach. In the error analysis of the mixed-dedicated lanes policies, the proportions α_ξ ($\xi = \{nv, av\}$) adopt the measured ME values obtained from the experiments.

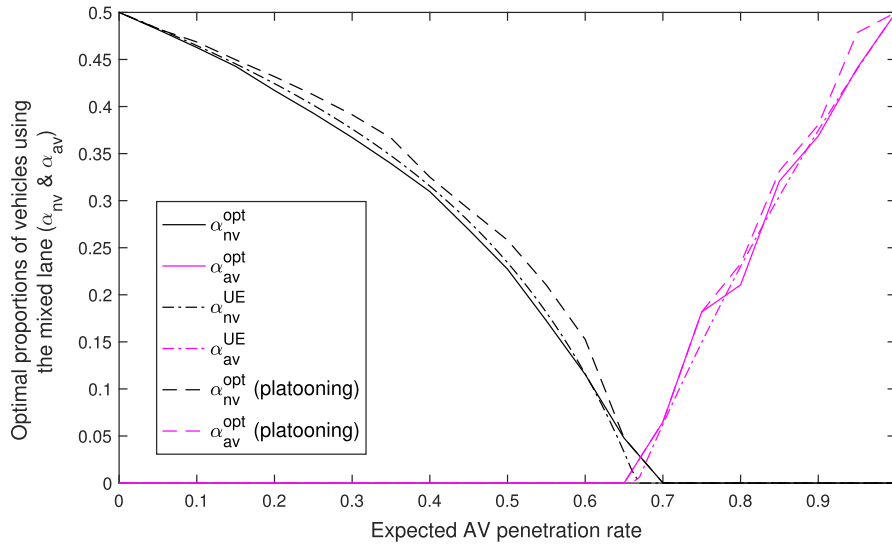


Fig. 7. Comparison of optimal α_{nv} and α_{av} obtained from three criteria for various penetration rates of AVs: (i) minimizing the delay of the approach following (O1), and (ii) the user-equilibrium values obtained from (28), and (iii) minimizing the delay as in method (i) with platooning of AVs. The traffic satisfies Assumptions [A] and [B] with the following signal timings: $C = 80$ [sec], $R = 40$ [sec], and $L = 0$.

Optimizing α_ζ to minimize the total delay of the approach can be achieved by solving the following optimization program:

$$\begin{aligned} \underset{\alpha_\zeta^{\text{opt}}}{\text{minimize}} \quad & D_k^{m-\zeta}(\alpha_\zeta^{\text{opt}})|_{\bar{k}=|n_{ap}|} \quad \zeta \in \left\{ \text{nv, av} \right\} \\ & 0 \leq \alpha_\zeta^{\text{opt}} \leq 1 \end{aligned} \tag{O1}$$

To compare the optimal proportions, α_ζ , derived from the two proposed methods, a numerical study was performed for an approach fulfilling Assumptions [A] and [B] and with the signal timings as $C = 80$ [sec], $R = 40$ [sec], and $L = 0$. The resulting optimal proportions α_ζ^{UE} and $\alpha_\zeta^{\text{opt}}$ are shown for various EPRs in Fig. 7. It can be seen that the optimal proportions that minimize the delay, i.e. $\alpha_\zeta^{\text{opt}}$, are almost equal to the UE proportions, α_ζ^{UE} . Hence, the UE condition is a near-optimum candidate. Moreover, both methods advise zero proportion of NVs (AVs) to use the mixed lane in the mixed-NV (mixed-AV) lanes policy for $p \geq 0.70$ ($p \leq 0.65$). In other words, if more than 70% of the road users in the mixed-NV lanes policy or less than 65% of them in the mixed-AV lanes policy are AVs, the optimal lane allocation strategy is the dedicated lanes policy.

The effect of platooning of AVs on $\alpha_\zeta^{\text{opt}}$ is further demonstrated in Fig. 7, where the saturation flow of the mixed traffic refers to the best arrangement of vehicles in the stream. It is observed that platooning of AVs allows using higher proportions of AVs in the mixed lane, due to increase in the capacity of the mixed lane.

5.2. Lane management policy

The proposed delay models for various policies further enable us to optimize the lane management of a two-lane arterial road in real-time, and thus maximize the efficiency of the traffic signal in reducing the delay at the intersection. The proposed optimal lane management algorithms can be extended to a multi-lane motorway or arterial, which is a future research direction. As long as the approach remains undersaturated, it is conjectured and justified through observations of numerical studies that the arrival flow and the signal timing at the intersection have little influence on the optimal lane management policy. Accordingly, the optimal lane management policy mainly is a function of the following listed factors that directly influence the saturation flow of each lane: (i) The EPR of AVs, (ii) the principal headway components h_{i-j} ($i, j \in \{\text{nv, av}\}$), (iii) the proportions α_ξ ($\xi = \{\text{nv, av}\}$) for the mixed-dedicated lanes policies, and (iv) platooning of AVs.

The delay of a two-way signalized approach with Assumptions [A] and [B] with $C = 80$ [sec], $R = 40$ [sec], and $L = 0$, and adopting different lane management policies are plotted for various EPRs in Fig. 8(a). The mixed lanes in each policy adopt the general arrangement of vehicles, and the mixed-dedicated lanes policies take optimal proportions α_ξ^{opt} and UE proportions α_ξ^{UE} . The figure confirms that the two alternative proportions α_ξ in the mixed-dedicated lanes policy return similar delays. In other words, the finding indicates that the drivers naturally enforce the optimal proportions to equalize the flow over capacity ratios of both lanes. This finding is crucial from the practical perspective, since NVs cannot be directly controlled by the Traffic Management Centre to change lanes in the mixed-NV lanes policy.

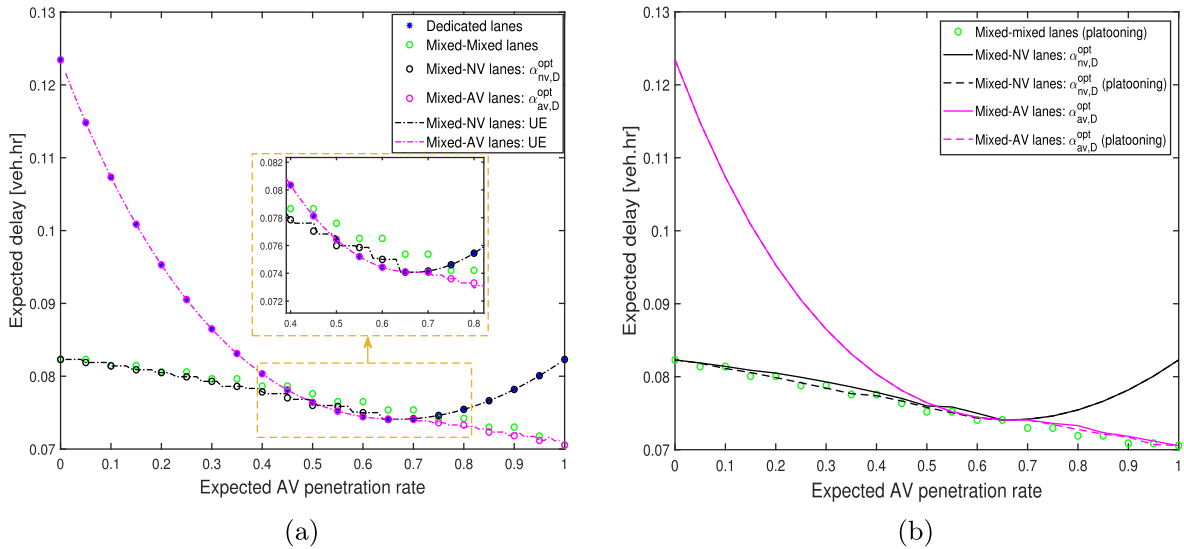


Fig. 8. (a) Comparison of the total vehicle delays for a two-lane approach complying with Assumptions [A] and [B] with $C = 80$ [sec], $R = 40$ [sec], and $L = 0$. The delays are obtained from the proposed models adopting the following policies: (1) the dedicated lanes; (2) the mixed-mixed lanes; (3) the mixed-NV lanes with optimal proportions α_{nv}^{opt} and α_{nv}^{UE} ; (4) the mixed-AV lanes with optimal proportions α_{av}^{opt} and α_{av}^{UE} . Vehicles in the mixed lanes follow the general arrangement. (b) Studying the effect of platooning of AVs on the delay of lane management policies including at least one mixed lane for various EPRs.

The results further indicate that the mixed-mixed lanes policy with stochastic arrangement of vehicles returns near optimal delays for all the EPR ranges, particularly for low and high EPRs. Quantitatively, this translates to less than 2% reduction in delays when using the mixed-NV lanes policy instead of the mixed-mixed lanes policy for EPRs less than 50%. Analogously, less than 2% reduction in delays are attained from using the mixed-AV lanes in lieu of the mixed-mixed lanes policy for EPRs higher than 50%. In summary, given headway components defined in Assumption [A], under the general (stochastic) arrangement of vehicles in the mixed lanes the best lane-allocation policy is: (I) the mixed-NV lanes policy for $0\% \leq EPR \leq 50\%$; (II) the dedicated lanes policy for $50\% < EPR < 65\%$; and (III) the mixed-AV lanes policy for $65\% \leq EPR \leq 100\%$. Note that the mixed-dedicated lanes policies are equivalent to the mixed-mixed lanes under 0% and 100% penetration rate of AVs.

The effect of platooning of AVs on the optimal lanes policy for minimizing the delay is demonstrated in Fig. 8(b). It can be seen that minor improvements are observed for the mixed-dedicated lanes policies after implementing the platooning of AVs. More importantly, the figure highlights that if the technology facilitates the AVs to be platooned, the mixed-mixed lanes policy becomes the optimal policy for minimizing the delay of the approach for the whole range of AV EPR.

6. Summary, conclusions, and future works

This paper has analytically derived the average and standard deviation of headway of a mixed traffic stream with autonomous and human-driven vehicles considering the expected penetration rate of AVs and arrangement of vehicles in the traffic stream. Microsimulation results have affirmed the accuracy of the developed models, despite ignoring the stochasticity of headways between AVs and NVs. The total delay of a two-lane road with interrupted mixed traffic has been analytically formulated based on the proposed saturation flow models for the mixed traffic with various lane management policies: (i) dedicated lanes, (ii) mixed-mixed lanes, (iii) mixed-NV lanes, and (iv) mixed-AV lanes. The accuracy of the established delay models has been justified employing microsimulation experiments.

Moreover, optimal proportions of the dedicated vehicle types in the mixed-dedicated lanes policies have been obtained based on two alternative criteria: (a) minimizing the delay and (b) the queueing-delay user equilibrium. We have shown that the methods are fairly equivalent, indicating that the traffic intrinsically adjusts the proportions in an optimal way.

The key conclusions from the study are: (1) the developed analytical models for the average headway of the mixed traffic are almost invariant to the moderate variabilities of individual headways and the AV penetration rate, and (2) the established delay models are invariant to Assumptions [I-V] demonstrated in Section 4.6. Therefore, the developed analytical formulas for estimating the saturation flow, and delay of the mixed traffic, provide a reliable and effective tool in improving the traffic management policies for the next generation of automated transportation systems. The models can be applied to real world traffic conditions with a desirable accuracy, instead of detailed microsimulation models with excessive computation time.

Future research direction is to analyze and model jointly the longitudinal and lateral dynamics of AVs in the mixed flow as an integrated model. Moreover, future research will focus on the integrated traffic signal optimization and optimal lane management of multi-lane arterials serving a mixed traffic, together with addressing the spillback phenomena. A natural extension then is to investigate the network-level analysis of mixed traffic and considering street-allocation to different type of vehicles.

Acknowledgment

This research was partly supported by Early Career Researcher Development funding by the University of Sydney, Faculty of Engineering and Information Technologies. The authors are indebted to Joao Aguiar Machado, Alexander Skabardonis, and Nikolas Geroliminis for their contributions towards the initiation of this research.

Appendix A. Properties of the average headway and delay models

Proposition 1. *Provided that Assumption [H0] is satisfied, the average headway models (3), (6), and (8) are decreasing and concave functions of the AV penetration rates.*

Proof. We first prove the statement for the best and worst arrangements, and then generalize it to the general arrangement. Differentiating $\bar{h}_k^{\text{best}}(n)$ defined in (8) with respect to the penetration rate (i.e. with respect to k , as n is a constant) results in $(h_{\text{av-av}} - h_{\text{nv-nv}})/(n - 1)$, which is less than or equal to zero (from Assumption [H0]). Similarly, differentiating $\bar{h}_k^{\text{worst}}(n)$ defined in (6) with respect to k , results in $(h_{\text{nv-av}} + h_{\text{av-nv}} - 2h_{\text{nv-nv}})/(n - 1)$ for $k/n < 0.5$ and $(-h_{\text{nv-av}} - h_{\text{av-nv}} + 2h_{\text{av-av}})/(n - 1)$ for $k/n > 0.5$, which both are less than or equal to zero. Hence, both of these functions are strictly decreasing when $h_{\text{nv-nv}} > h_{\text{av-av}}$. Moreover, the second derivative of $\bar{h}_k^{\text{best}}(n)$ with respect to k is zero, thus it is both a convex and a concave function of the penetration rate. To add, the second derivative of $\bar{h}_k^{\text{worst}}(n)$ is zero, except at $k/n = 0.5$, wherein in limit this derivative is $2(h_{\text{av-av}} - h_{\text{nv-nv}})$ that is less than or equal to zero. Accordingly, from the properties of convex functions, one can conclude that the average headways $\bar{h}_k^{\text{best}}(n)$ and $\bar{h}_k^{\text{worst}}(n)$ are both decreasing and concave functions of the penetration rate (Boyd and Vandenberghe, 2004).

The headway of the general arrangement is the average of the headways of all the possible combinations of having k AVs in the platoon. It is clear that the average headway of every other combination of k AVs in total of n vehicles is a concave and decreasing function of the penetration rate, k/n , that belongs to the set $[\bar{h}_k^{\text{best}}(n), \bar{h}_k^{\text{worst}}(n)]$. Conclusively, from Boyd and Vandenberghe (2004), $\bar{h}_k^{\text{general}}(n)$ is also a decreasing and concave function of the penetration rate. □

Proposition 2. *The simplified headway models (9) approximate the accurate models (2), (5), and (7) with the following precisions ($\bar{k} = \lfloor np \rfloor$):*

- i. $\bar{h}_{\bar{k}}^{\text{best}}(n) - E[\bar{h}^{\text{best}}(k, n)] = 0$,
- ii. $0 \leq \bar{h}_{\bar{k}}^{\text{worst}}(n) - E[\bar{h}^{\text{worst}}(k, n)] \leq \frac{n}{n-1}(h_{\text{nv-nv}} + h_{\text{av-av}} - h_{\text{av-nv}} - h_{\text{nv-av}}) + \frac{1}{n-1}(h_{\text{av-nv}} - h_{\text{av-av}})$,
- iii. $0 \leq \bar{h}_{\bar{k}}^{\text{general}}(n) - E[\bar{h}^{\text{general}}(k, n)] \leq \max_{\gamma} \left\{ \gamma h_{\text{nv-nv}} + (1 - \gamma)h_{\text{av-av}} - \frac{A(1-\gamma)n(n)H}{(n-1)C_n^{(1-\gamma)n}} \right\}$, where $0 \leq \gamma \leq 1$.

Proof. From (8), $\bar{h}_k^{\text{best}}(n)$ is a linear function of the AV penetration rate, thus Item (i) holds. Moreover, from Proposition 1, $\bar{h}_k^{\text{worst}}(n)$ is concave function of the AV penetration rate. Hence, from Simic (2009) we have

$$0 \leq \bar{h}_{\bar{k}}^{\text{worst}}(n) - E[\bar{h}^{\text{worst}}(k, n)] \leq \bar{h}_0^{\text{worst}}(n) + \bar{h}_n^{\text{worst}}(n) - 2\bar{h}_{0.5n}^{\text{worst}}(n),$$

which implies the statement of Item (ii). For the general arrangement a more generalized inequality established in Simic (2009) is employed to obtain a tighter upper-bound for the headway estimation error:

$$0 \leq \bar{h}_{\bar{k}}^{\text{general}}(n) - E\left[\bar{h}^{\text{general}}\left(k, n\right)\right] \leq \max_{\gamma} \left[\gamma \bar{h}_0^{\text{general}}(n) + (1 - \gamma)\bar{h}_n^{\text{general}}(n) - \bar{h}_{(1-\gamma)n}^{\text{general}}(n) \right],$$

which implies the statement of Item (iii). □

Proposition 3. *The simplified delay models (26) approximate the accurate models (17), (19), (22), and (24) with the following precisions ($\bar{k} = \lfloor n_a p \rfloor$ and $\zeta = \{m - m, m - \text{nv}, m - \text{av}\}$):*

$$\inf_k \{h^{\text{nv-av}}(k, \bar{k})\} n_a p \left(1 - p\right) \leq E\left[D^{\text{nv-av}}\left(k, n_a\right)\right] - D_{\bar{k}}^{\text{nv-av}} \leq \sup_k \{h^{\text{nv-av}}(k, \bar{k})\} n_a p \left(1 - p\right), \tag{A.1}$$

$$|E[D^{\zeta}(k, n_a, \cdot)] - D_{\bar{k}}^{\zeta}(\cdot)| \leq 2n_a p \left(1 - p\right) \sup_{k \neq \bar{k}} \left\{ \frac{|D_{\bar{k}}^{\zeta}(\cdot) - D_{\bar{k}}^{\zeta}(\cdot)|}{2(k - \bar{k})^2} \right\} \tag{A.2}$$

where $h^{\text{nv-av}}\left(k, \bar{k}\right) := \frac{D_k^{\text{nv-av}} - D_{\bar{k}}^{\text{nv-av}}}{(k - \bar{k})^2} - \frac{D_{\bar{k}}^{\text{nv-av}}}{k - \bar{k}}$, $\dot{D}_k^{\text{nv-av}} := dD_k^{\text{nv-av}}/dk$, and the undefined argument “ \cdot ” in $D^{\zeta}(k, n_a, \cdot)$ is empty for $\zeta = \{m - m\}$, α_{nv} for $\zeta = \{m - \text{nv}\}$, and α_{av} for $\zeta = \{m - \text{av}\}$.

Proof. We first prove the estimated delay bounds for the dedicated lanes policy. It can be shown from (18) that $D_k^{\text{nv-av}}$ is a differentiable and a convex function of the penetration rate as its second derivative is positive (see Fig. A.9(a)). Therefore, it can be shown that the Jensen’s gap for $D_k^{\text{nv-av}}$, fulfills (A.1) (see Liao and Berg, 2018).

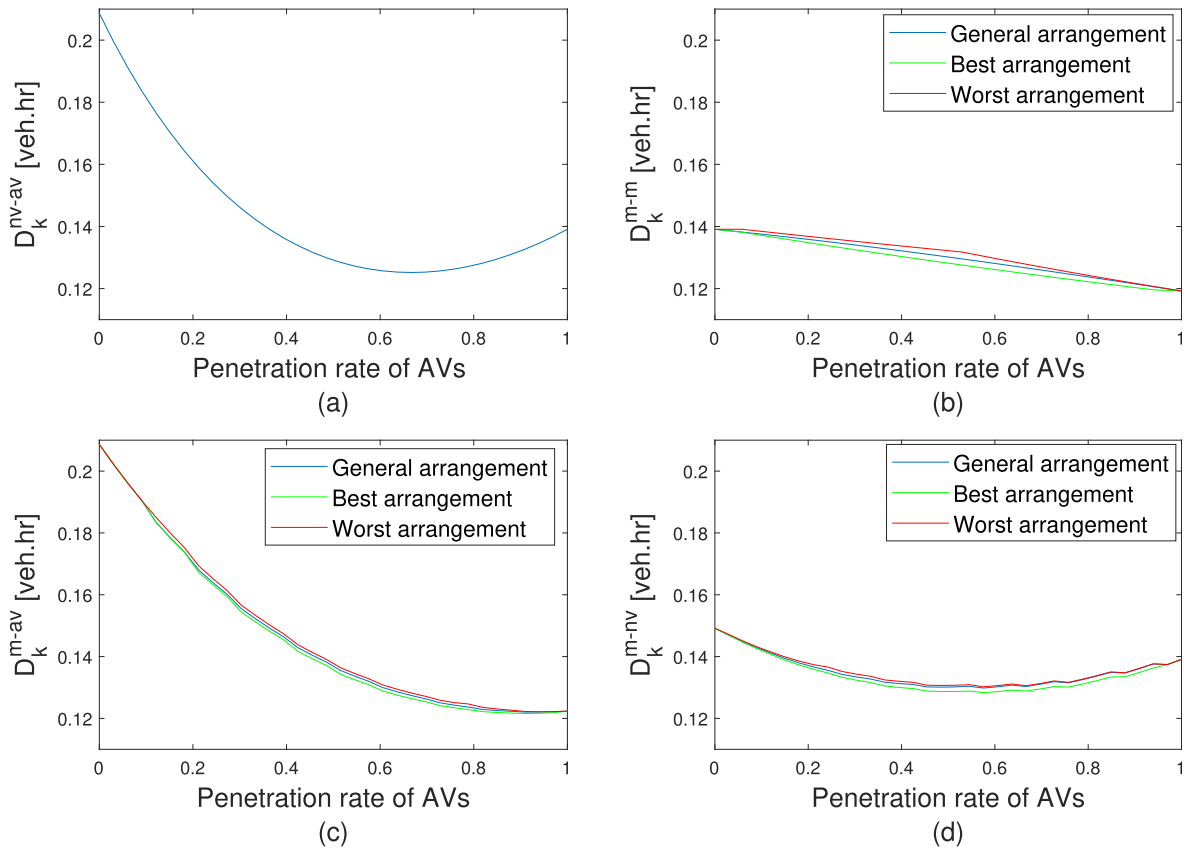


Fig. A.9. Total delay of a two-lane approach for various AV penetration rates and lane management policies ($\alpha_{av} = 0.3$ and $\alpha_{nv} = 0.3$). Arrival flow of the approach is $Q^a = 1000$ [veh/h], cycle time is $C = 120$ [sec], loss-time is $L = 2$ [sec] and red time facing the approach is $R = 50$ [sec]. The general, best, and worst arrangements of vehicles are considered for the mixed lanes. (For interpretation of the references to color in this figure legend, the reader is referred to the web version of this article.)

Despite the dedicated lanes policy, the delay functions for the other policies are not differentiable, nor convex (see Fig. A.9(b-d)). However, from (20), (23), and (25), those functions are 2-Hölder continuous and their growth rates are not faster than k^2 . Hence, the estimation error bounds (A.2) are straightforwardly obtained from Theorem 1 in Gao et al. (2017). \square

Remark 3. Note that the upper-bounds given in Propositions 2 and 3 can be improved using more advanced estimation techniques. Finding tighter upper-bounds for the Jensen’s gap is an active area of research.

Appendix B. Description of parameters in (28)

$$\begin{aligned}
 a_0^{nv} &= (b_2 + b_1 + b_0)p^2 + h_{nv-nv}p(p - 1), \\
 a_1^{nv} &= -h_{nv-nv}(p - 1)^2 - (2b_0 + b_1 + h_{nv-nv})p(p - 1), \\
 a_2^{nv} &= (b_0 + h_{nv-nv})(p - 1)^2, \\
 a_0^{av} &= (b_2 + b_1 + b_0 + h_{av-av})p^2, \\
 a_1^{av} &= -h_{av-av}p^2 - (2b_0 + b_1 + h_{av-av})p(p - 1), \\
 a_2^{av} &= (b_2 + b_1 + b_0 + h_{av-av})p^2.
 \end{aligned}$$

References

Ali, Y., Zheng, Z., Haque, M.M., Wang, M., 2019. A game theory-based approach for modelling mandatory lane-changing behaviour in a connected environment. *Transp. Res. Part C: Emerg. Technol.* 106, 220–242.
 Arem, B.V., Driel, C.J.G.V., Visser, R., 2006. The impact of cooperative adaptive cruise control on traffic-flow characteristics. *IEEE Trans. Intell. Transp. Syst.* 7 (4), 429–436.
 Argote-Cabañero, J., Christofa, E., Skabardonis, A., 2015. Connected vehicle penetration rate for estimation of arterial measures of effectiveness. *Transp. Res. Part C*

- Emerg. Technol. 60, 298–312.
- Boyd, S., Vandenberghe, L., 2004. *Convex Optimization*. Cambridge University Press.
- Chandler, D., 1987. *Introduction to Modern Statistical Mechanics*. Oxford University Press, Oxford.
- Chen, D., Ahn, S., Chitturi, M., Noyce, D.A., 2017. Towards vehicle automation: roadway capacity formulation for traffic mixed with regular and automated vehicles. *Transp. Res. Part B: Methodol.* 100, 196–221.
- Friedrich, B., 2016. *The Effect of Autonomous Vehicles on Traffic*. Springer, Berlin, Heidelberg, pp. 317–334.
- Gao, X., Sitharam, M., Roitberg, A.E., 2017. **Bounds on the jensen gap, and implications for mean-concentrated distributions.** eprint arXiv: 1712.05267.
- Ghiasi, A., Hussain, O., Qian, Z., Li, X., 2017. A mixed traffic capacity analysis and lane management model for connected automated vehicles: a markov chain method. *Transp. Res. Part B: Methodol.* 106, 266–292.
- Gong, S., Du, L., 2018. Cooperative platoon control for a mixed traffic flow including human drive vehicles and connected and autonomous vehicles. *Transp. Res. Part B: Methodol.* 116, 25–61.
- Han, Y., Chen, D., Ahn, S., 2017. Variable speed limit control at fixed freeway bottlenecks using connected vehicles. *Transp. Res. Part B: Methodol.* 98, 113–134.
- Hyland, M., Mahmassani, H.S., 2018. Dynamic autonomous vehicle fleet operations: optimization-based strategies to assign avts to immediate traveler demand requests. *Transp. Res. Part C: Emerg. Technol.* 92, 278–297.
- Ilgın Guler, S., Menendez, M., Meier, L., 2014. Using connected vehicle technology to improve the efficiency of intersections. *Transp. Res. Part C: Emerg. Technol.* 46, 121–131.
- Jia, D., Ngoduy, D., 2016. Platoon based cooperative driving model with consideration of realistic inter-vehicle communication. *Transp. Res. Part C: Emerg. Technol.* 68, 245–264.
- Lamotte, R., de Palma, A., Geroliminis, N., 2017. On the use of reservation-based autonomous vehicles for demand management. *Transp. Res. Part B: Methodol.* 99, 205–227.
- Li, P.Y., Shrivastava, A., 2002. Traffic flow stability induced by constant time headway policy for adaptive cruise control vehicles. *Transp. Res. Part C: Emerg. Technol.* 10 (4), 275–301.
- Li, R., Liu, X., Nie, Y., 2018a. Managing partially automated network traffic flow: efficiency vs. stability. *Transp. Res. Part B: Methodol.* 114, 300–324.
- Li, Y., Tang, C., Li, K., Peeta, S., He, X., Wang, Y., 2018b. Nonlinear finite-time consensus-based connected vehicle platoon control under fixed and switching communication topologies. *Transp. Res. Part C: Emerg. Technol.* 93, 525–543.
- Liao, J.G., Berg, A., 2018. Sharpening jensen's inequality. *Am. Stat.* 1–4.
- Mohajerpoor, R., Saberi, M., Ramezani, M., 2017. Delay variability optimization using shockwave theory at an undersaturated intersection. *IFAC-PapersOnLine* 50(1), 5289 – 5294, 20th IFAC World Congress.
- Mohajerpoor, R., Saberi, M., Ramezani, M., 2019. Analytical derivation of the optimal traffic signal timing: minimizing delay variability and spillback probability for undersaturated intersections. *Transp. Res. Part B: Methodol.* 119, 45–68.
- Pan, T., Lam, W.H.K., Sumalee, A., Zhong, R., 2019. Multiclass multilane model for freeway traffic mixed with connected automated vehicles and regular human-piloted vehicles. *Transportmetrica A: Transp. Sci.* 1–29.
- Qian, Z., Li, J., Li, X., Zhang, M., Wang, H., 2017. Modeling heterogeneous traffic flow: a pragmatic approach. *Transp. Res. Part B: Methodol.* 99, 183–204.
- Ramezani, M., Machado, J.A., Skabardonis, A., Geroliminis, N., 2017. Capacity and delay analysis of arterials with mixed autonomous and human-driven vehicles. In: *2017 5th IEEE International Conference on Models and Technologies for Intelligent Transportation Systems (MT-ITS)*, pp. 280–284.
- Ramezani, M., Ye, E., 2019. Lane density optimisation of automated vehicles for highway congestion control. *Transportmetrica B: Transp. Dyn.* 7 (1), 1096–1116.
- Simic, S., 2009. On an upper bound for jensen's inequality. *J. Inequal. Pure Appl. Math.* 10 (2), 5.
- Stern, R.E., Cui, S., Delle Monache, M.L., Bhadani, R., Bunting, M., Churchill, M., Hamilton, N., Haulcy, R., Pohlmann, H., Wu, F., Piccoli, B., Seibold, B., Sprinkle, J., Work, D.B., 2018. Dissipation of stop-and-go waves via control of autonomous vehicles: field experiments. *Transp. Res. Part C: Emerg. Technol.* 89, 205–221.
- Sun, J., Zheng, Z., Sun, J., 2018. Stability analysis methods and their applicability to car-following models in conventional and connected environments. *Transp. Res. Part B: Methodol.* 109, 212–237.
- Talebpoor, A., Mahmassani, H.S., 2016. Influence of connected and autonomous vehicles on traffic flow stability and throughput. *Transp. Res. Part C: Emerg. Technol.* 71, 143–163.
- Tilg, G., Yang, K., Menendez, M., 2018. Evaluating the effects of automated vehicle technology on the capacity of freeway weaving sections. *Transp. Res. Part C: Emerg. Technol.* 96, 3–21.
- Tuchner, A., Haddad, J., 2017. Vehicle platoon formation using interpolating control: a laboratory experimental analysis. *Transp. Res. Part C: Emerg. Technol.* 84, 21–47.
- van den Berg, V.A.C., Verhoef, E.T., 2016. Autonomous cars and dynamic bottleneck congestion: the effects on capacity, value of time and preference heterogeneity. *Transp. Res. Part B: Methodol.* 94, 43–60.
- Yang, D., Zheng, S., Wen, C., Jin, P.J., Ran, B., 2018. A dynamic lane-changing trajectory planning model for automated vehicles. *Transp. Res. Part C: Emerg. Technol.* 95, 228–247.
- Yu, C., Feng, Y., Liu, H.X., Ma, W., Yang, X., 2018. Integrated optimization of traffic signals and vehicle trajectories at isolated urban intersections. *Transp. Res. Part B: Methodol.* 112, 89–112.
- Zhao, W., Ngoduy, D., Shepherd, S., Liu, R., Papageorgiou, M., 2018. A platoon based cooperative eco-driving model for mixed automated and human-driven vehicles at a signalised intersection. *Transp. Res. Part C: Emerg. Technol.*
- Zhou, Y., Ahn, S., Chitturi, M., Noyce, D.A., 2017. Rolling horizon stochastic optimal control strategy for ACC and CACC under uncertainty. *Transp. Res. Part C: Emerg. Technol.* 83, 61–76.
- Zhou, Y., Ahn, S., Wang, M., Hoogendoorn, S., 2019. Stabilizing mixed vehicular platoons with connected automated vehicles: an H-infinity approach. *Transp. Res. Part B: Methodol.*